Journal of Thermal Science Vol.30, No.4 (2021) 1108−1115

https://doi.org/10.1007/s11630-020-1358-3 **Article ID: 1003-2169(2021)04-1108-08**

Characteristics of Preheating Combustion of Power Coal with High Coking Properties

ZHANG Yi[1,2], ZHU Jianguo[1,2*], LYU Qinggang[1,2], PAN Fei[1,2], ZHU Shujun[1,2]

1. Institute of Engineering Thermophysics, Chinese Academy of Sciences, Beijing 100190, China
2. University of Chinese Academy of Sciences, Beijing 100049, China

© Science Press, Institute of Engineering Thermophysics, CAS and Springer-Verlag GmbH Germany, part of Springer Nature 2020

Abstract: Yankuang coal with the high coking property is difficult to use through direct combustion. The main purpose of this paper is to study the combustion characteristics and NO_x emissions of this type of coal using preheating combustion technology. The experimental results show that after the pulverized coal is preheated, the char residue characteristic is significantly reduced from 5 to 1. During the preheating process, the preheating temperature is stable at about 910°C, and the particle size of char after preheating is reduced, and the pore structure and specific surface areas are increased. The combustion temperature of preheated fuel is stable at around 1100°C, and the combustion efficiency can reach more than 99% under different conditions. Changing the structure of the secondary air nozzles during the preheating combustion process can influence the characteristics of NO_x emissions. The NO_x emission of the central nozzle is about 112 mg/Nm^3 lower than that of the annular nozzle. Changing the tertiary air distribution modes can reduce the final NO_x emissions to 215 mg/Nm^3 (@6% O_2), and the corresponding conversion ratio of fuel N to the final NO_x is 4.2%. The results of this experiment prove that the Yankuang coal can achieve stable combustion by preheating combustion technology, and this proposed a new way for the utilization of Yankuang coal.

Keywords: Yankuang coal, coking properties, preheating combustion, NO_x emissions

1. Introduction

Coal is the most important energy resource in China. According to statistics from 2018, coal consumption accounts for 59% of total energy consumption, decreased by 1.4% from 2017, but the current situation, with coal being a main energy, will not change for a long period of time [1].

There are many types of coal in China, one of which is coking coal. In China's new coal classification (GB5751-86), 1/2 medium caking coal, gas coal, gas-fat coal, fat coal, 1/3 coking coal, meagre coal, lean coal, etc., are all belonged to the category of coking coal. Because these coals have good coking properties, they can be used as coking or coal blending [2–4]. Generally, the coking properties for power coal (including the char residue characteristic and cohesive index) are relatively low. For example, the char residue characteristic of Shenmu bituminous coal is 0, and the cohesive index is 0. However, the Yankuang bituminous coal studied in this paper has the advantages of high volatile matter, low ash content and high calorific value, but some characteristics, such as the char residue characteristic of 5, the cohesive index of 25, and the Roga index of 30, restrict the direct

Received: Aug 11, 2019 AE: TIAN Zhenyu Corresponding author: ZHU Jianguo E-mail: zhujianguo@iet.cn

combustion of Yankuang coal. Here, the char residue characteristic refers to the shape of the remaining material after thermal decomposition of coal. According to different shapes, it is divided into 8 serial numbers, and the serial number is the characteristic code of char residue. It is generally considered that No. 1 and No. 2 have no adhesion; No. 3 and No. 4 have weak adhesion, and No. 5 to No. 8 have strong adhesion [14]. At present, there are few studies on such a coal with high char residue characteristic. Shinichi Miura† studied the variations of pore structure after viscous coalification [5]; Bao Junfeng studied the coking properties of coking coal [6]; FU Xinmin studied the pyrolysis characteristics and kinetic behaviors of coking coal [7]. There are few reports on the combustion characteristics of this type of coal.

Institute of Engineering Thermophysics of the Chinese Academy of Sciences proposed a new process for realizing high efficient and clean combustion with wide coal type adaptability [8, 9]. A series of studies have been carried out using this new process. The coal types involved mainly include bituminous coal and anthracite, which all have low char residue characteristic in the range of 0 to 2. The experimental results show that the preheating combustion, an extremely promising advanced combustion technology [10–13], has obvious advantage with low NO_x emissions.

Therefore, in order to use this type of coal with high char residue characteristic efficiently, Yankuang coal with the char residue characteristic of 5 is used to study the combustion and NO_x emission characteristics by preheating combustion technology.

2. Experiments

2.1 Apparatus and methods

This experiment was performed on a 30 kW preheated combustion test rig. The process of the experimental system is shown in Fig. 1. During the preheating process, both the fuel and air with low excess air coefficient are sent to the circulating fluidized bed (CFB) for partial gasification and combustion, which preheat the remaining fuel to above 800°C. The preheating process is accompanied by the formation of high temperature coal gas and preheated char. The high temperature coal gas and preheated char can be called as preheated fuel. The preheated fuel enters the down-fired combustor (DFC) through the horizontal tube and mixes with the secondary air and the tertiary air to be burned out.

The CFB riser has a diameter of 78 mm and a height of 1500 mm. The horizontal pipe is 48 mm in diameter with a length of 500 mm. A sampling port is settled in the middle of the horizontal pipe to sample and analyze the preheated coal gas and the preheated char. The DFC is 260 mm in inner diameter with a height of 3000 mm. Two secondary air nozzles are arranged at the top of the DFC: a central and an annular. A schematic diagram of the secondary air nozzles structure is shown in Fig. 2. The tertiary air can be fed separately or combined at the same time at the positions of 200 mm, 600 mm, 1200 mm below the nozzle, respectively.

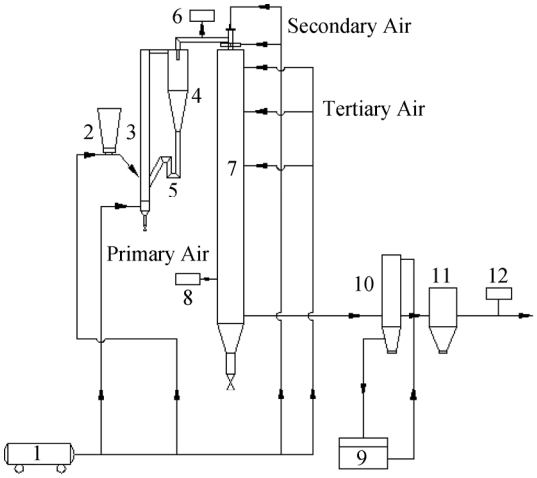

1. Air Compressor, 2. Screw Feeder, 3. Riser, 4. Cyclone, 5. U-valve, 6. Sampling Port, 7. Down-fired Combustor 8. Sampling Port, 9. Water Tank, 10. Water Tank, 11. Bag Filter, 12. Gas Analyzer

Fig. 1 Schematic diagram of the test system

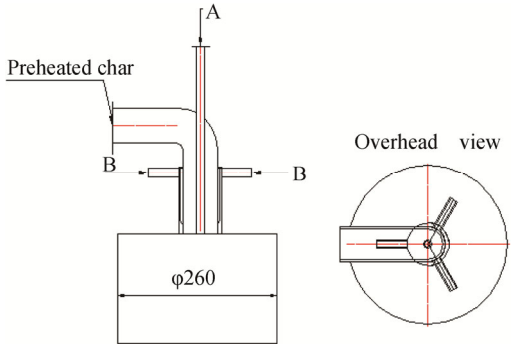

Fig. 2 The structure of secondary air nozzles (A is the central nozzle, B is the annular nozzle)

Four (Ni-Ci/Ni-Si) thermocouples were installed in the CFB: three of them are at 100 mm, 500 mm, 1450 mm above the air distribution plate for measuring the riser temperature, and another is at the return leg. Five (Pt/Pt-Rh) thermocouples were arranged at 100 mm, 400 mm, 900 mm, 1400 mm, and 2400 mm below the nozzle. The accuracy of the thermocouple is within ±0.5%.

The O_2 concentration along the CFB outlet and the DFC can be measured online using the KM9106 analyzer. Other gases in the DFC include NO, NO_2, N_2O, CO, CO_2, H_2O, NH_3, and HCN, can be measured by GASMET FTIR DX-4000. According to the manufacturer's specifications, the instrument error is within ±2%.

Table 1 Proximate and ultimate analysis of fuel

Items	Proximate analysis/%				Ultimate analysis/%					Low calorific value/MJ·kg^{-1}
	M_{ad}	A_{ad}	V_{ad}	FC_{ad}	C_{ad}	H_{ad}	N_{ad}	S_{ad}	O_{ad}	$Q_{net,ad}$
Yankuang coal	0.6	14.2	29.75	55.45	65.77	4.97	1.31	0.42	11.84	26.36

Table 2 Coking properties of Yankuang coal

Yankuang coal	Coking index	Thickness of colloidal matter layer	Maximum Gieseler fluidity/ddpm	The char residue characteristic	Roga index
Values	25	8	4	5	25

2.2 Fuel characteristics

The studied coal is Yankuang coal, and its proximate analysis and elemental analysis are shown in Table 1. The content of nitrogen, the volatile matter and the calorific value are high. The coking properties of Yankuang coal are shown in Table 2 below. The char residue characteristic is high and the cohesive index is large. The maximum fluidity of the colloid is rotated at a larger angle, and the maximum thickness of the colloidal layer is larger [14]. The particle size distribution range of Yankuang coal is 0 mm to 0.355 mm, as is shown in Fig. 3. The corresponding mean particle size of cumulative volume fraction of 50%, 90% is 103.5 μm and 296.195 μm, respectively.

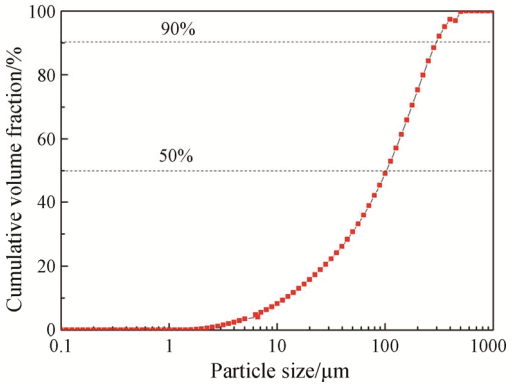

Fig. 3 The particle size distribution diagram of Yankuang raw coal

2.3 Experimental conditions

In order to carry out the corresponding research, seven cases are designed, including changing the secondary air nozzle structures and the tertiary air distribution modes. The operating parameters of different cases are shown in Table 3. Among them, Case 2 and Case 3 are set to study the effect of different secondary air nozzle structures, and Cases 1, 3, 4, 5, 6, and 7 are set to study the effect of different tertiary air distribution modes. In Table 3, λ_{CFB} is the CFB air equivalence ratio; λ is the total excess air coefficient; λ_{se} is the secondary air equivalence ratio; λ_{te200}, λ_{te600} and λ_{te1200} are the equivalence ratios of 200 mm, 600 mm, 1200 mm from the top of the DFC. The formula is as follows.

Table 3 Operating parameters of different cases

Case	Nozzle structures	λ_{CFB}	λ_{se}	λ_{te200}	λ_{te600}	λ_{te1200}	λ
1	central	0.41	0.31	0.173	0.173	0.173	1.24
2	annular	0.41	0.31	0.26	0.26	0	1.24
3	central	0.41	0.31	0.26	0.26	0	1.24
4	central	0.41	0.31	0.26	0	0.26	1.24
5	central	0.41	0.31	0	0.26	0.26	1.24
6	central	0.41	0.31	0	0	0.52	1.24
7	central	0.41	0.31	0	0.52	0	1.24

$$\lambda_{CFB} = \frac{A_{pr} + A_{re} + A_{ca}}{A_{stoic}} \quad (1)$$

$$\lambda_{se} = \frac{A_{se}}{A_{stoic}} \quad (2)$$

$$\lambda_{te200} = \frac{A_{te200}}{A_{stoic}} \quad (3)$$

$$\lambda_{te600} = \frac{A_{te600}}{A_{stoic}} \quad (4)$$

$$\lambda_{te1200} = \frac{A_{te1200}}{A_{stoic}} \quad (5)$$

$$\lambda = \lambda_{CFB} + \lambda_{se} + \lambda_{te200} + \lambda_{te600} + \lambda_{te1200} \quad (6)$$

where A_{stoic} (Nm^3/h) is the gas flow rate with stoichiometric complete burnout. A_{pr}, A_{re}, A_{ca} and A_{se} are the air flow rates of the primary air, returning air, carrying coal air and secondary air. While A_{te200}, A_{te600} and A_{te1200} are the tertiary air flow rates at 200 mm, 600 mm, 1200 mm below the nozzle, respectively.

In this study, the parameters of CFB were kept constant: λ_{CFB} was maintained at 0.41, and λ_{se} was maintained at 0.31. Only the secondary air nozzle structure and the tertiary air distribution modes were changed, while λ remains unchanged at 1.24.

According to the principle of the ash balance, the conversion ratios of components in fuel, C_X, during the preheating were calculated by the following formula [15]:

$$C_X = 1 - \frac{A_1 \times X_2}{A_2 \times X_1} \tag{7}$$

where A_1 and A_2 are the ash contents in the fuel and preheated fuel, respectively, and X_1 and X_2 are the contents of component X in the fuel and the preheated fuel, respectively.

3. Results and Discussion

3.1 Preheating characteristics of CFB

During the experiment, the CFB equivalence ratio was maintained at 0.41. The temperature distribution of each measuring point of CFB is shown in Fig. 4. It can be seen that the CFB runs smoothly under different cases. The average temperature of the bottom, middle and upper portions of the riser is regarded as the preheating temperature, which is stable at (910±10)°C.

Analyzing the preheated char at the outlet of the CFB shows that the char residue characteristic is 1, while the char residue characteristic of raw coal is 5. This result indicates that the preheating process can reduce the char residue characteristic of coal. According to Eqs. (1)–(7), the conversion ratio of each component can be calculated, and the results are shown in Table 4.

It can be seen from Table 4 that the carbon conversion ratio is close to 50%, indicating that 50% of the carbon is released during the preheating process, and the remaining 50% of carbon was sent to the DFC together with the preheated coal gas. Almost all of the volatiles and most of the hydrogen, oxygen and nitrogen elements are released in the CFB. About 51.21% of the sulfur element is released during the preheating process, and the remaining sulfur elements are released in the DFC.

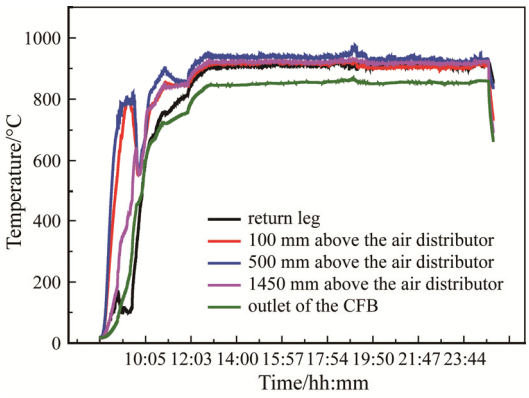

Fig. 4 Temperature distributions of CFB

As shown in Fig. 5, by comparing the particle size distribution of the preheated char and the raw coal, it can be seen that the particle size of the preheated char has a decrease compared with the raw coal. The maximum particle sizes of the raw coal cumulative volume fraction of 50%, 90% were 103.05 μm and 296.20 μm, respectively. The maximum particle sizes of the preheated char cumulative volume fraction of 50%, 90% were 13.48 μm and 56.67 μm, respectively. There are three main reasons for the decreased particle size: Firstly, the heating rate of the riser is fast, leading to the formation of the hot spring force and the crush of the raw coal; Secondly, due to the local gasification reaction occurs, part of the gases escape from the inner hole of coal; Thirdly, larger particle size is separated by the separator in the preheating process.

The apparent morphologies of the raw coal and preheated char are shown in Fig. 6. It is obvious that the surface of the raw coal is smooth and dense. In addition, the structure is compact and the pore structure is substantially invisible with extremely low degree of fragmentation. While the surface of the preheated char is rough and porous with high degree of fragmentation, the coal particles are broken into many small particles. These results are consistent with the results of the distribution of particle size above.

According to the measurement results of the specific surface area, the specific surface area of the raw coal is 1.36 m^2/g, and the preheated char is 1.98 m^2/g, which is 1.45 times of the raw coal. The result indicates that the specific surface area can be increased by preheating process. The heat exchange between preheated char and the outside can be increased after the specific surface area is increased, which have a favorable effect on the diffusion and adsorption of oxygen and combustion products. However, for coals with low char residue characteristic, the specific surface area of preheated char is generally more than three times of raw coal [16]. This may be due to the fact that the Yankuang coal is more

Table 4 Proximate and ultimate analysis of preheated char

Items	Proximate analysis/wt%				Ultimate analysis/wt%					Low calorific value/MJ·kg^{-1}
	M_{ad}	A_{ad}	V_{ad}	FC_{ad}	C_{ad}	H_{ad}	N_{ad}	S_{ad}	O_{ad}	$Q_{net,ad}$
Preheated char	0.56	29.8	4.34	65.3	69.14	1.6	0.54	0.43	2.62	24.28
Conversion ratio/%	55.53	0	93.05	43.88	49.91	84.66	80.36	51.21	81.21	

viscous, and the particles are easily agglomerated. Some of the pores formed during the preheating process are blocked due to viscosity, and the increasing amplitude of the specific surface area is greatly reduced.

In summary, the temperature of preheating process is stable. Compared to the raw coal, the particle size of preheating char is decreased; the specific surface area and pore structure are increased, and the char residue characteristic is lowered. The above analysis results indicate that the preheating process has a modification and upgrading effect on the fuel.

3.2 Temperature distributions in DFC

Throughout the experiment, the CFB equivalence ratio and the secondary air equivalence ratio were maintained at 0.41 and 0.31, respectively. Only the secondary air nozzle structures and the tertiary air distribution modes were changed, and the effects of different cases on the temperature distribution of the DFC were observed as shown in Fig. 7 and Fig. 8.

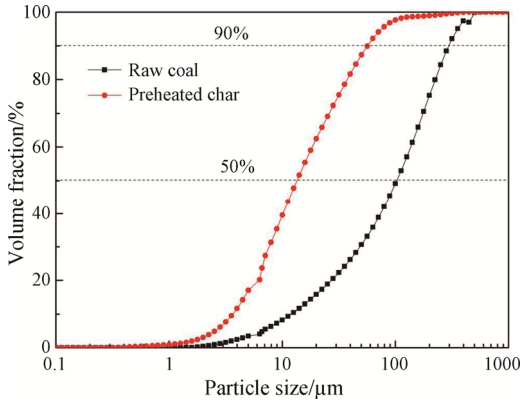

Fig. 5 The particle size distribution of raw coal and preheated char

It can be seen from Fig. 7 that the maximum temperature values of the two secondary air nozzle structures are at 400 mm below the nozzle. The maximum temperature of the annular nozzle is 1066°C, which is 14°C higher than the maximum temperature of the central nozzle. The temperature at 100 mm below the nozzle for annual nozzle is 44°C higher than that of the central nozzle, which indicates that the fuel and air are mixed and combusted at the 100 mm and 400 mm below the nozzle more uniformly and intensely under the annular nozzle structure. The combustion efficiencies of the central nozzle and the annular nozzle were 99.5% and 98.6%, respectively.

The structure of the secondary air nozzle keeps the same, and only the different tertiary air distribution modes were changed. The temperature distribution along the DFC is shown in Fig. 8. “200+600+1200” means that the tertiary air is evenly fed from 200 mm, 600 mm, 1200 mm below the nozzle. “600+1200” means that the tertiary air is evenly fed from 600 mm, 1200 mm below the nozzle, and other combinations are similar.

It can be seen from Fig. 8 that the variations of tertiary air distribution modes will result in the appearance of the maximum temperature at different positions along the DFC. For example, when the tertiary air distribution mode adopts “200+600+1200”, “200+600”, “200+1200”

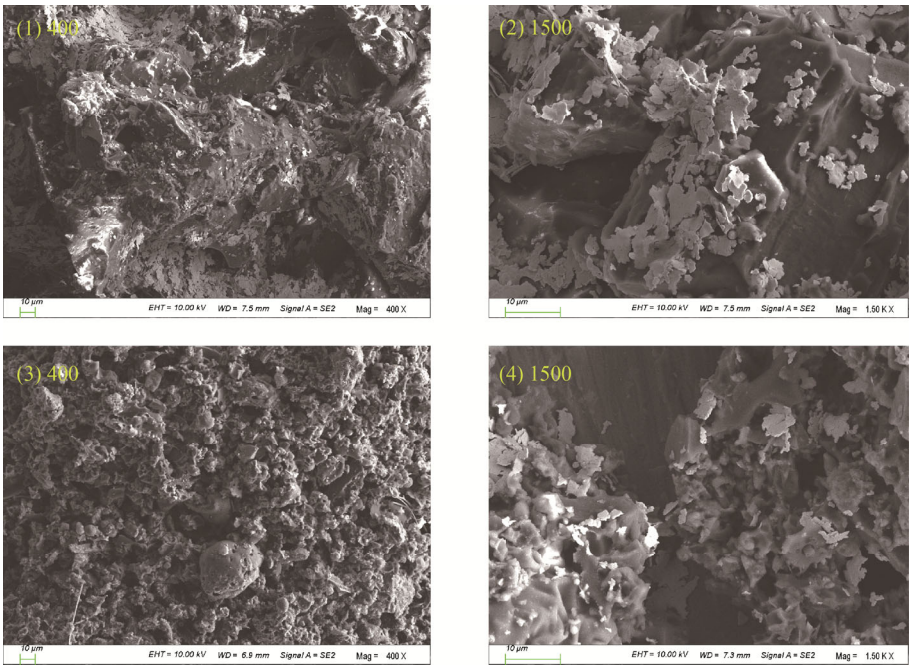

Fig. 6 The morphology comparison diagram of Yankuang coal before and after preheating. (1) and (2) are raw coal; (3) and (4) are preheated char; 400 and 1500 respectively represent the magnification times)

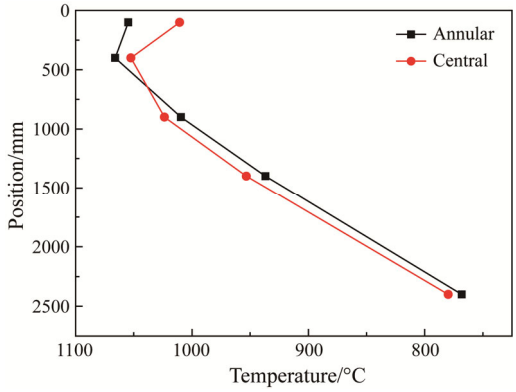

Fig. 7 Temperature distributions along the centerline of DFC with different secondary nozzle structures

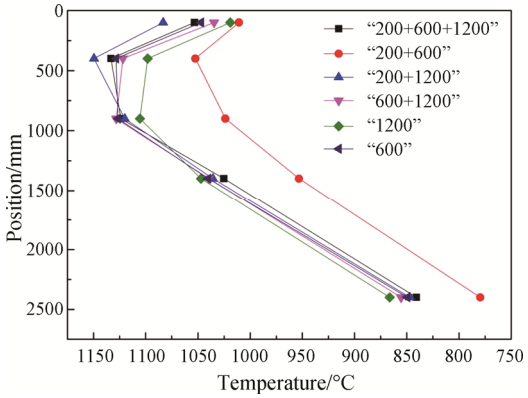

Fig. 8 Temperature distributions along the centerline of the DFC when the tertiary air feeding position was changed

and "600", the maximum temperature point appears at 400 mm below the nozzle. The maximum temperature point appears at 900 mm below the nozzle when the tertiary air distribution modes are "600+1200" and "1200". This indicates that different tertiary air distribution modes have a great influence on the temperature distribution of the DFC.

There are several reasons to explain this phenomenon. First of all, the main reason is that the temperature of preheated char is higher than its ignition temperature after preheating, but cannot reach the complete combustion after feeding the secondary air. Therefore, when the tertiary air is fed from different positions, the combustion conditions at different positions are changed, resulting in the change of temperature distribution. When the tertiary air distribution mode adopts "200+600+1200", "200+600", "200+1200" and "600", the fuel and air are mixed best at 400 mm below the nozzle, and combustion reaction is the most intense. Therefore, the maximum temperature appears at 400 mm below the nozzle. However, when the tertiary air distribution modes are "600+1200" and "1200", the most intense position of combustion reaction is around 900 mm below the nozzle, so the maximum temperature point appears at 900 mm below the nozzle. Above all, adjusting the temperature of different positions in the DFC can be achieved by rationally organizing the distribution of the tertiary air.

3.3 NO_x emissions of different cases

3.3.1 The influence of different secondary air nozzle structures on NO_x emissions

The structure change of the secondary air nozzle will affect the temperature distributions of the DFC and the mixing mode of the preheated char and the air. Ultimately, the final NO_x emission is affected. The NO_x emissions of the two secondary air nozzle structures are shown in Fig. 9. As can be seen from Fig. 9, when the secondary air nozzle is changed from the annular to the central, the final NO_x emissions is reduced from 660 mg/Nm^3 to 548 mg/Nm^3 (@6% O_2).

Some reasons can be given to illustrate the results. Firstly, when the secondary air was fed from the central nozzle, the air was fed from the center, and the preheated char is wrapped outside the air; when the secondary air was entered from the annular nozzle, the preheated char was fed in the middle position, and the air was wrapped outside the preheated char. The mixture method of former between fuel and air is beneficial to reduce NO_x emissions. Secondly, it can be seen from the literature [17] that the reduction of NO in the region of CFB outlet to 100 mm below the nozzle has a great influence on the NO_x emissions throughout the combustion process. Therefore, the lower temperature of the central nozzle at 100 mm and 400 mm compared to the annular nozzle is another reason for the difference in NO_x emissions between the two nozzle structures. Thirdly, the secondary air injection velocity with central nozzle is smaller than the annular nozzle, resulting that the residence time of fuel and air in the furnace with central nozzle was longer than the annular nozzle. Therefore, more NO_x was reduced in the central nozzle than the annular nozzle.

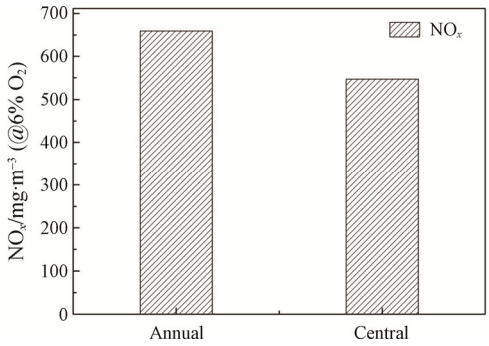

Fig. 9 NO_x emissions of different secondary air nozzle structures in the final gases

Yanyao's research shows that the NO formation at 100 mm below the nozzle mainly from the oxidation of NH_3 in the combustion process, and the secondary air nozzles can effectively suppress this part of NO [18]. The result is the same as the results of this paper: different secondary air nozzles have effects on NO_x emissions. Therefore, in combination with the above analysis, it is possible to adjust the final NO_x emissions by optimizing the secondary air nozzle structures.

3.3.2 The influence of different tertiary air distribution modes on NO_x emissions

This paper, when the secondary air was entered from the central nozzle, explores the effect of the variations of tertiary air distribution modes on the final NO_x emissions. Taking Case 1, Case 3, Case 4 and Case 6 as examples, the experimental results are shown in Fig. 10.

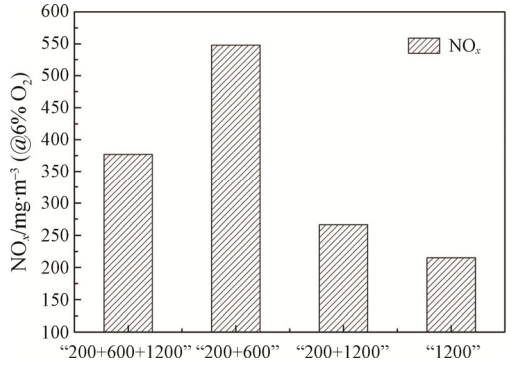

Fig. 10 The NO_x emissions of different tertiary air distribution modes

Different tertiary air distribution modes have a great influence on NO_x emissions, but have little effect on combustion efficiency. The combustion efficiency of all cases in this experiment is above 98%. When the tertiary air was fed from different positions, the mixing ratios of air and fuel at different measuring points along the DFC were different, resulting in different combustion intensity. As Zhu's research shows, different tertiary air distributions will affect the length of the reduction zone along the DFC. The longer the reduction zone, the longer the residence time of the fuel in the reduction zone, and the greater the reduction of NO_x, and the lower the NO_x emissions [19–21]. In this experiment, the length of reduction zone with the tertiary air distribution mode adopting "200+600" is the shortest, followed by the modes of "200+600+1200" and "200+1200", and the mode of "1200" is the longest. Therefore, the NO_x emissions of the tertiary air distribution mode adopting "200+600" is the highest, followed by the modes of "200+600+1200" and "200+1200", and the mode of "1200" is the lowest.

The minimum NO_x emission that can be achieved by different tertiary air distribution modes is 215 mg/Nm^3 (@6% O_2). According to the ratio of actual NO_x emissions value and the total theoretical emissions of fuel nitrogen to NO_x, the actual conversion ratio of fuel nitrogen to NO_x can be calculated and the value is 4.2%.

4. Conclusions

In this paper, the preheating characteristics, combustion characteristics and NO_x emissions characteristics of Yankuang coal with high coking properties are studied. According to the experimental results, the following conclusions can be concluded:

(1) From the experimental results, preheating combustion technology can reduce the char residue characteristic of this type of coal with high coking properties and achieve stable combustion.

(2) Compared with the raw coal, the preheated char has smaller particle size, more pore structure, larger specific surface area and lower char residue characteristic.

(3) Different secondary air nozzle structures and tertiary air distribution mode has a great effect on NO_x emissions in the flue gas. The NO_x emissions from the central nozzle are 112 mg/Nm^3 lower than that of the annular nozzle. Different tertiary air distribution modes mainly change the final NO_x emissions by changing the length of reduction zone along the DFC. The different tertiary air distribution modes can achieve NO_x emissions as low as 215 mg/Nm^3 (@6% O_2). The corresponding conversion ratio of fuel nitrogen to NO_x was 4.2%.

In summary, the coal with high char residue characteristic and high viscosity can achieve stable and high-efficient combustion by preheating combustion, and this proposes a new way for the utilization of Yankuang coal.

Acknowledgement

This study is supported by the National Natural Science Foundation of China (No. 51676187).

References

[1] National Bureau of Statistics of People's Republic of China. China Statistical Yearbook-2019, Beijing, China Statistics Press, 2019. (in Chinese)

[2] Han L.P., Research on the char residue characteristic of coking coal in kailuan. China new technology and new products, 2009(18): 119. (in Chinese)
DOI: 10.13612/j.cnki.cntp.2009.18.017.

[3] Zhang S.Q., Coal chemistry. 4th Edition, China University of Mining and Technology Press, 2015. (in Chinese)

[4] Shen M.X., Resources and utilization of coking coal in China. Chemical Industry Press, 2007. (in Chinese)
[5] Miura S., Silveston P.L., Change of pore properties during carbonization of coking coal. Carbon, 1980, 18(2): 93–108.
[6] Bao J.F., Xue G.F., Zhan L.Z., et al., Evaluation index of the char residue characteristic of coking coal. Fuel & Chemical Processes, 2014, 45(2): 5–7. (in Chinese)
[7] Fu X.M., Zhang Y.X., Guo Z.Y., et al., Characteristics and kinetics of the pyrolysis of coking coal tailings. Journal of China Coal Society, 2013, 38(2): 320–325. (in Chinese)
[8] Lyu Q.G., Zhu J.G., Pulverized coal combustion and NO_x emissions in high temperature air from circulating fluidized bed. Proceedings of the CSEE, 2007, (32): 7–12. (in Chinese)
[9] Lyu Q.G., Zhu J.G., Niu T.Y., Pulverized coal high temperature preheating method. Beijing: CN101158468, Chinese patent, 2007. (in Chinese)
[10] Zhu J.G., Experimental study on pulverized coal combustion and NO_x emissions in high temperature air with low oxygen concentration. University of Chinese Academy of Sciences, Beijing, China, 2008. (in Chinese)
[11] Wang J., Experimental study on combustion and NO_x emissions of pulverized anthracite preheated by circulating fluidized bed. University of Chinese Academy of Sciences, Beijing, China, 2011. (in Chinese)
[12] Yao Y., Experimental study on preheated combustion characteristics and NO_x emission of pulverized semi-coke. University of Chinese Academy of Sciences, Beijing, China, 2016. (in Chinese)
[13] Ouyang Z.Q., Experimental study on preheating and combustion characteristics and pollutants emission of pulverized anthracite. University of Chinese Academy of Sciences, Beijing, China, 2014. (in Chinese)
[14] Chen P., Nature classification and utilization of coal in China, Chemical Industry Publisher, Beijing, China, 2007, pp. 201–238, 445–460. (in Chinese)
[15] Zhu J.G., Yao Y., Lyu Q.G., et al., Experimental investigation of gasification and incineration characteristics of dried sewage sludge in a circulating fluidized bed. Fuel, 2015, 150: 441–447.
[16] Nie X., Zhou Z.J., Lyu M., et al., Experimental study on pulverized coal flow ignition and flameout in high temperature air. Proceedings of the CSEE, 2008, 28(14): 67–72. (in Chinese)
[17] Yang E.H., Zhu J.G., Ouyang Z.Q., Lyu Q.G., Experimental study on the relationship between particle characteristics and nitrogen release during fine powder semi-coke preheating combustion. Proceeding of the CSEE, 2017, 37(15): 4415–4421, 4582. (in Chinese)
[18] Yao Y., Zhu J.G., Ouyang Z.Q., et al., Experimental study on nitrogen migration characteristics during fine powder semi-coke preheating combustion process. Proceedings of the CSEE, 2016, (8): 2188–2194. (in Chinese)
[19] Ouyang Z.Q., Zhu J.G., Lyu Q.G., Experimental study on combustion characteristics and NO_x emissions characteristics of anthracite powder after preheating in circulating fluidized bed. Proceeding of the CSEE, 2014, 34(11): 1748–1754. (in Chinese)
[20] Zhu S.J., Lyu Q.G., Zhu J.G., et al., Effect of air distribution on NO_x emissions of pulverized coal and char combustion preheated by a circulating fluidized bed. Energy & Fuels, 2018, 32(7): 7909–7915.
[21] Zhu S.J., Lyu, Q.G., Zhu, J.G., et al., Experimental study on NO_x emissions of pulverized bituminous coal combustion preheated by a circulating fluidized bed. Journal of the Energy Institute, 2019, 92(2): 247–256.